



# APPLICATIONS OF A HYBRID METHOD TO A PLATE WITH SIMPLY SUPPORTED BOUNDARY CONDITIONS

Claire Churchill<sup>1\*</sup>      Joshua Meggitt<sup>1</sup>      Daniel Wong-McSweeney<sup>1</sup>  
 Trevor Cox<sup>1</sup>      James Woodcock<sup>2</sup>

<sup>1</sup> Acoustics Research Centre, University of Salford, Manchester, M5 4WT, UK

<sup>2</sup> Arup, 6<sup>th</sup> Floor, 3 Piccadilly Place, Manchester, M1 3BN, UK

## ABSTRACT

The EN12354 building acoustics prediction standards are based on the statistical energy analysis (SEA) method. In a traditional SEA path analysis, lightweight or heavyweight materials have different principal paths that determine the sound insulation for the specified building acoustics frequency range (50Hz-5000Hz). Different building materials require different applications of the engineering method (EN12354) to determine in-situ sound insulation with flanking. A hybrid method, such as the (finite element method) FEM-SEA hybrid approach, offers an alternative theoretical framework to predict in situ sound insulation with the capacity to combine vastly different methods. In a hybrid model, different power flow contributions (due to the deterministic and direct-field energies) are naturally separated into different matrices. This work investigates the feasibility of using a hybrid model to predict sound insulation. The hybrid method is applied to three different materials. These models are compared against traditional SEA and infinite plate models.

**Keywords:** *sound insulation (SI), hybrid model, building acoustics.*

## 1. INTRODUCTION

Statistical energy analysis (SEA) is a well-known method to calculate the sound insulation of different materials. It is the basis upon which the EN12354 building acoustics prediction

standards are written. This work investigates the feasibility of using an alternative theoretical framework, the hybrid model, to calculate coupling loss factors and predict sound insulation. In this work we compare a hybrid approach against calculations made using traditional SEA and infinite plate models. Three different material models are investigated. Section 2 describes the plate specifications and the room properties. The coupling loss factors calculated using a hybrid approach are compared with a traditional SEA method. The sound insulation is also calculated using traditional SEA and infinite plate models and compared with the results from the hybrid method. These methods are described in section 3. Finally, sections 4 and 5 present the results and conclusion of the early study.

## 2. DESCRIPTION OF THE MODEL

### 2.1 Model overview

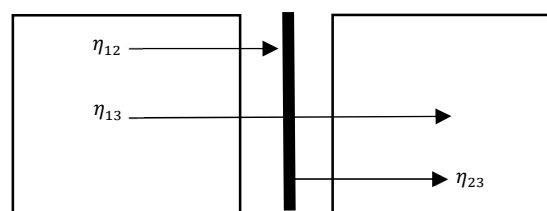


**Figure 1.** Two acoustic volumes separated by a flat plate [1].

\*Corresponding author: [c.e.churchill@salford.ac.uk](mailto:c.e.churchill@salford.ac.uk)

**Copyright:** ©2023 First author et al. This is an open-access article distributed under the terms of the Creative Commons Attribution 3.0 Unported License, which permits unrestricted use, distribution, and reproduction in any medium, provided the original author and source are credited.

The model comprises three subsystems; two acoustic volumes are separated by a flat plate (see Fig. 1). The acoustic volumes are modelled as two acoustic half spaces and the plate is modelled using both infinite plate and analytic techniques. A direct field approach is used to model the infinite plate and a modal model of a plate with simply supported edges is used to model the deterministic plate system. These methods are combined to give the coupling loss factors and hence the sound insulation of the system.

## 2.2 Plate specifications

**Table 1.** Plate properties.

|                                      | CLT                  | Steel                 | Perspex             |
|--------------------------------------|----------------------|-----------------------|---------------------|
| Elastic modulus (Nm <sup>-1</sup> )  | 1.58×10 <sup>9</sup> | 2.10×10 <sup>11</sup> | 5.6×10 <sup>9</sup> |
| Poisson ratio                        | 0.3                  | 0.3                   | 0.3                 |
| Dimensions (m <sup>2</sup> )         | 3.6×3.6              | 0.5×0.5               | 0.91×0.91           |
| Surface density (kgm <sup>-3</sup> ) | 37.9                 | 39.3                  | 11.6                |
| Thickness (m)                        | 0.12                 | 0.005                 | 0.0098              |
| Internal loss factor (-)             | 0.01                 | 0.01                  | 0.02                |

The study examples are three square plates (small to large). The properties of the plates are listed in table 1. The steel plate is also modelled in [1].

## 2.3 Room specifications

The rooms are assumed to be air filled with typical gas constants for air at room temperature (see table 2). For the infinite plate models, the plate and room dimensions are not considered. In the SEA model the calculation for the cross laminated timber (CLT) was performed with typical room volumes for dwellings with large rooms (59.4 m<sup>3</sup> and 54.0 m<sup>3</sup>); the steel with typical room volumes for dwellings with very small rooms (both 10.0 m<sup>3</sup>); and the Perspex has typical room volumes for dwellings with small and large rooms (27.0 m<sup>3</sup> and 54.0 m<sup>3</sup>). In the hybrid model the source and receiving rooms were assumed to be the same volume both 10.0 m<sup>3</sup>. To simplify the comparison with the hybrid model in all of the calculations the rooms are described by a loss factor that does not vary over the frequency range; this can be calculated from the reverberation time of the rooms. The

value 0.01 is typical of a reverberation time of 0.44s at 500 Hz. Note in real world applications it is usually only possible to measure the total loss factor of a room or cavity.

**Table 2.** Room properties.

|                                    | Room A | Room B |
|------------------------------------|--------|--------|
| Gas Density (kgm <sup>-3</sup> )   | 1.205  | 1.205  |
| Speed of sound (ms <sup>-1</sup> ) | 343    | 343    |
| Loss factor (-)                    | 0.01   | 0.01   |

## 3. METHOD

The loss factors were determined using the hybrid method and, for comparison, a traditional SEA method. In all models the material is assumed to be isotropic, and the plates are square with equidistant grid spacing. The minimum mesh requirements for all dynamic stiffness matrices were calculated and the highest minimum mesh requirement used to perform the calculation at each frequency. A variable mesh density that increased with increasing frequency was implemented to work around speed and memory constraints.

### 3.1 Loss factors determined by the hybrid method

#### 3.1.1 No deterministic system (i.e. $D_p=0$ )

The coupling loss factors using the hybrid method were determined by [1, 2, 3]:

$$\eta_{jk} = \left( \frac{2}{\omega \pi n_j} \right) \sum_{r,s} \text{Im}\{\mathbf{D}_{\text{dir},rs}^{(j)}\} (\mathbf{D}_{\text{tot}}^{-1} \text{Im}\{\mathbf{D}_{\text{dir}}^{(k)}\} \mathbf{D}_{\text{tot}}^{-1*T})_{r,s} \quad (1)$$

Where  $n_j$  is the modal density of subsystem  $j$ ,  $\mathbf{D}_{\text{dir},rs}^{(j)}$  is the  $(r, s)$  term of the direct field dynamic stiffness matrix of subsystem  $j$ , and  $\mathbf{D}_{\text{dir}}^{(k)}$  is the direct field dynamic stiffness matrix of subsystem  $k$ , the subscripts  $r$  and  $s$  indicate the  $(r, s)$  term and  $\mathbf{D}_{\text{tot}}$  is given by

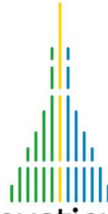
$$\mathbf{D}_{\text{tot}} = \sum_k \mathbf{D}_{\text{dir}}^{(k)} = \mathbf{D}_{\text{dir}}^{(1)} + \mathbf{D}_{\text{dir}}^{(2)} + \mathbf{D}_{\text{dir}}^{(3)} \quad (2)$$

$D_{\text{dir}} = 0$  therefore:

$$\omega \eta_{d,j} = 0 \quad (3)$$

and there is no deterministic system so:

$$P_{\text{in},j}^{\text{ext}} = 0 \quad (4)$$



### 3.1.2 Using the driving point dynamic stiffness for the deterministic system (i.e. $D_d = D_{point}$ )

The coupling loss factors are determined by Eqn. (1) but in this case [1].

$$\mathbf{D}_{tot} = \mathbf{D}_d + \sum_k \mathbf{D}_{dir}^{(k)} \quad (5)$$

In this approach the ensemble average of the deterministic dynamic stiffness matrix is given by the driving point dynamic stiffness of a plate.

$$E[\mathbf{D}_d] = \mathbf{D}_p \quad (6)$$

At the edges of the plate this is:

$$D_{p,edge} = i\omega\sqrt{B\rho h} \quad (7)$$

Where  $\omega$  is the angular frequency,  $B$  is the bending stiffness of the plate,  $\rho$  is the plate density, and  $h$  is the plate thickness. In the middle of a plate the driving point dynamic stiffness is:

$$D_{p,middle} = 8i\omega\sqrt{B\rho h} \quad (8)$$

There is no power directly input to the plate therefore Eqn. (4) is also applied.

### 3.1.3 Using a deterministic dynamic stiffness ( $D_d$ )

The coupling loss factors are determined by Eqns. (1) and (5) but in this approach the deterministic dynamic stiffness matrix is given by the matrix inverse of the sum of the modal contributions.

$$\mathbf{D}_d = \mathbf{H}_d^{-1} \quad (9)$$

The terms of  $H_d$  are given by [4]:

$$H_{d,jk} = \frac{4}{\rho ha^2} \sum_n \sum_m \frac{\sin^2 \frac{n\pi x_j}{a} \sin^2 \frac{m\pi y_k}{a}}{\omega_0^2 (1 + i\eta_p) - \omega^2} \quad (10)$$

Where  $a$  is the size of the square plate,  $\omega_0$  is the angular resonance frequency,  $\eta_p$  is the internal loss factor of the plate and  $n, m$  are integers. Similarly, to section 3.1.2 there is no power directly input to the plate therefore Eqn. (4) is also applied.

### 3.1.4 The direct field dynamic stiffness matrix ( $D_{dir}^{(2)}$ )

The direct field dynamic stiffness matrix is given by the matrix inverse of the receptance matrix [1]:

$$\mathbf{D}_{dir}^{(2)} = \mathbf{H}_{dir}^{-1} \quad (11)$$

The terms of  $H_{dir,jk}$  are given by [1]:

$$H_{dir,jk} = G(r_{jk}) \quad (12)$$

where  $G$  is the Green's function for the infinite plate and  $r_{jk}$  is the distance between grid points  $j$  and  $k$ . The Green's function is given by [1]:

$$G(r_{jk}) = (-i/8Bk^2)[H_0^{(2)}(kr_{jk}) - H_0^{(2)}(ikr_{jk})] \quad (13)$$

Where  $H_0^{(2)}$  is zeroth order the Hankel function of the second kind and  $k$  is the bending wave number.

### 3.1.5 The direct field dynamic stiffness matrix of the rooms ( $D_{dir}^{(0)}$ )

The direct field dynamic stiffness matrix of the rooms is given by [3]:

$$\mathbf{D}_{dir}^{(j)} = \frac{i8\pi\omega\rho ck_a^2}{k_s^4} \{\text{sinc}(k_a r) + if(k_a r)\} \quad (14)$$

where  $k_a$  is the acoustic wavenumber,  $k_s$  is the wavenumber corresponding to the grid spacing and

$$f(k_a r) = \frac{\cos(k_a r)}{k_a r} + \frac{1}{k_a r} \int_0^{k_s r / k_a} J_0(x) dx \quad (15)$$

and

$$r = \sqrt{(x - x_0)^2 + (y - y_0)^2} \quad (16)$$

where  $J_0(x)$  is a zeroth order Bessel function of the first kind. ( $\mathbf{D}_{dir}$  is undefined along the diagonal and is set to zero.)

The function is plotted where  $\{\text{sinc}(k_a r) + if(k_a r)\} > 0$ , this cut-off depends on the frequency resolution and mesh density. Langley [3] recommends four points per half wavelength; this was the mesh density implemented unless the modal mesh density requirement was higher. Also note the condition  $k_s \gg k_a$ , Wavenumbers which do not meet the condition  $k_s/k_a > 1$  are not included in the results.

### 3.1.6 Minimum mesh requirements

The minimum mesh requirements for each part of dynamic stiffness calculation were given by the maximum of: Six points per bending wavelength for the  $\mathbf{D}_d$  mesh, eight points per bending wavelength for the  $\mathbf{D}_{dir}^{(2)}$  mesh or eight points per acoustic wavelength for the  $\mathbf{D}_{dir}^{(1)}$  or  $\mathbf{D}_{dir}^{(3)}$  mesh. Grids no smaller than a 20x20 mesh were used.

### 3.2 Loss factors determined by a traditional SEA method

The coupling loss factors were determined by using the typical equations for a three-subsystem model [5, 6]. The radiation coupling is given by:

$$\eta_{ij} = \frac{\rho_0 c_0 \sigma}{\omega \rho h} \quad (17)$$

Where  $\rho_0$  is the gas density,  $c_0$  is the speed of sound of the gas,  $\sigma$  is the radiation efficiency given by Leppington et al. [7]. The plate is assumed to be simply supported and installed in an infinite baffle. The non-resonant coupling is given by:

$$\eta_{ij} = \frac{c_0 S}{4\omega V_i} \tau_{NR} \quad (18)$$

where  $S$  is the surface area of the plate,  $V_i$  is the volume of subsystem  $i$  and  $\tau_{NR}$  is the non-resonant transmission coefficient, given by Leppington et al. [8]. The modal densities of the plates are given by [5, 6]:

$$n_{B,p} = \frac{\pi f S}{c_{B,p}^2} \quad (19)$$

Where  $f$  is frequency and  $c_{B,p}$  is the bending wave phase velocity and the modal densities of the rooms are given by [5, 6]

$$n_R = \frac{4\pi f^2 V}{c_0^3} + \frac{\pi f S_T}{2c_0^2} + \frac{L_T}{8c_0} \quad (20)$$

where

$$S_T = 2(L_x L_y + L_x L_z + L_y L_z) \quad (21)$$

and

$$L_T = 4(L_x + L_y + L_z) \quad (22)$$

Where  $L_x$ ,  $L_y$  and  $L_z$  are the dimensions of the rooms.

### 3.3 Consistency relationship

The coupling loss factors can also be calculated or verified in the reverse direction using the consistency relationship. This is given by [5]:

$$\frac{\eta_{ij}}{n_j} = \frac{\eta_{ji}}{n_i} \quad (23)$$

## 4. RESULTS

### 4.1 Coupling loss factors

#### 4.1.1 No deterministic system (i.e. $D_d=0$ )

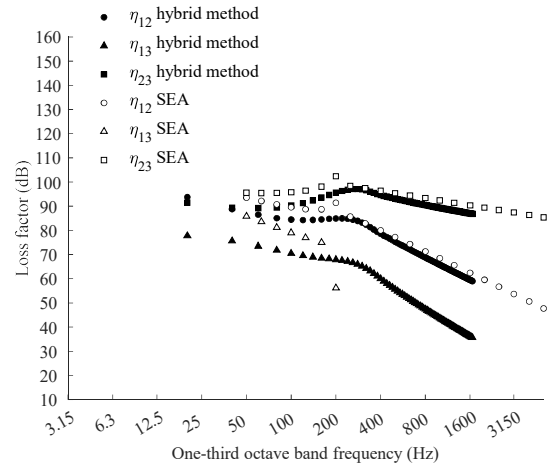


Figure 2. Coupling loss factors for the CLT plate.

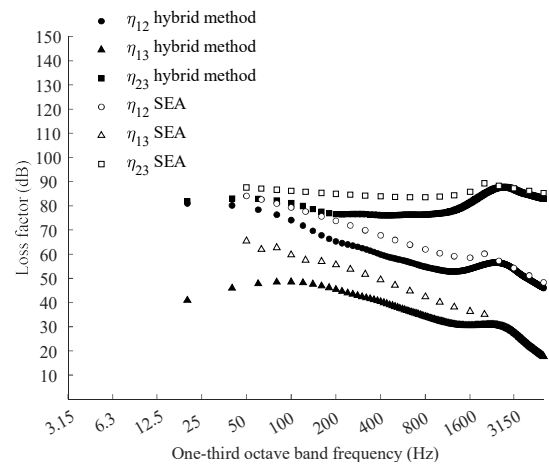
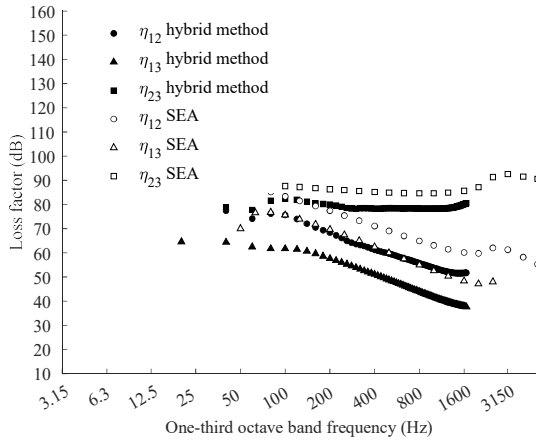


Figure 3. Coupling loss factors for the steel plate.



**Figure 4.** Coupling loss factors for the Perspex plate.

The different calculation methods to determine the coupling loss factors are compared in Figs. 2, 3 and 4. The  $\eta_{12}$  and  $\eta_{23}$  loss factors are replicated using the hybrid method, however unlike the traditional method a  $\eta_{13}$  loss factor is obtained over the whole frequency range (not just below the critical frequency,  $f_c$ ). The physical significance of the loss factor,  $\eta_{13}$  in this frequency range ( $f > f_c$ ) is unclear. Further work would be required to extend the upper frequency range of the hybrid model. Further work is also required to appropriately include the deterministic dynamic stiffness ( $D_d$ ) (see also section 4.1.2 and 4.1.3).

*4.1.2 Using the driving point dynamic stiffness (i.e.  $D_p = D_{point}$ )*

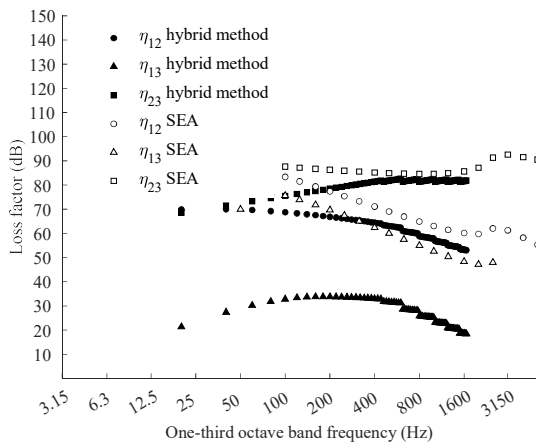


**Figure 5.** Coupling loss factors for the Perspex plate ( $D_p = D_{point}$ ).

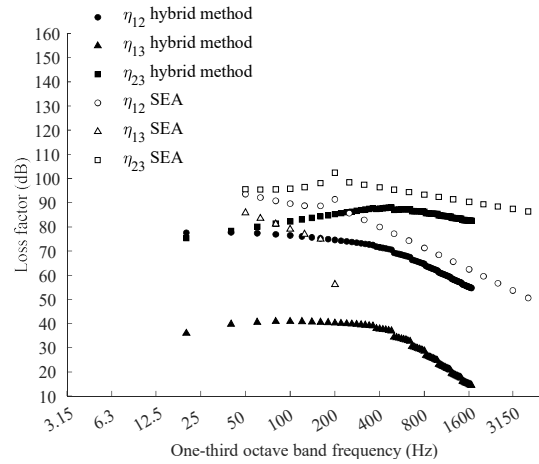


**Figure 6.** Coupling loss factors for the CLT plate ( $D_p = D_{point}$ ).

Preliminary efforts to incorporate a deterministic dynamic stiffness ( $D_d$ ) are shown in Figs. 5 and 6. The Agreement between the calculation methods is diminished. This is particularly true of the  $\eta_{13}$  loss factor for both plates.

*4.1.3 Using a deterministic dynamic stiffness ( $D_d$ )*

The coupling loss factors when incorporating a deterministic dynamic stiffness ( $D_d$ ) are shown in Fig. 7 and 8.

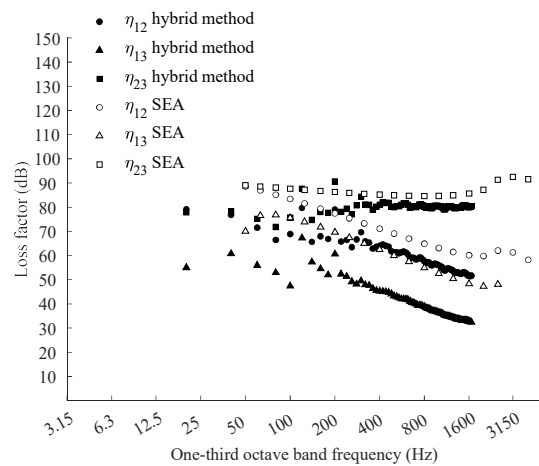


**Figure 7.** Coupling loss factors for the Perspex plate (including  $D_p$ ).

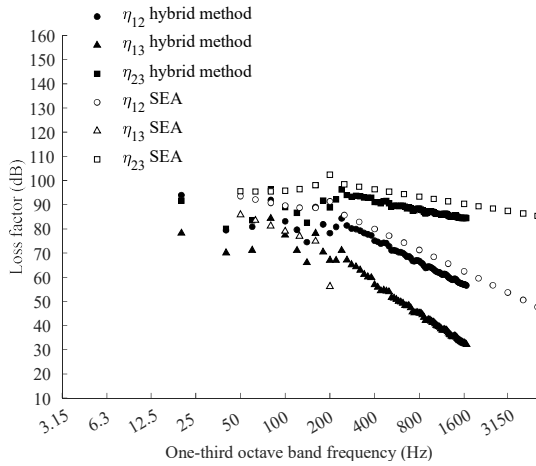
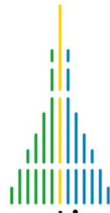


Figure 8. Coupling loss factors for the CLT plate (including  $D_p$ ).

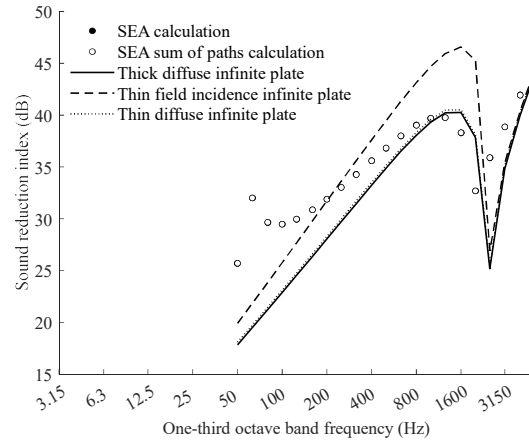


Figure 10. Sound insulation for the steel plate.

#### 4.2 Sound insulation

The results of the calculated sound insulation are shown in Figs. 9, 10 and 11. The sound insulation for the traditional SEA and the infinite plate models are presented; further work would be required to extend the upper frequency range of the hybrid model. The critical frequencies of the CLT, steel and Perspex plates are 423 Hz, 2393 Hz and 2898 Hz respectively.

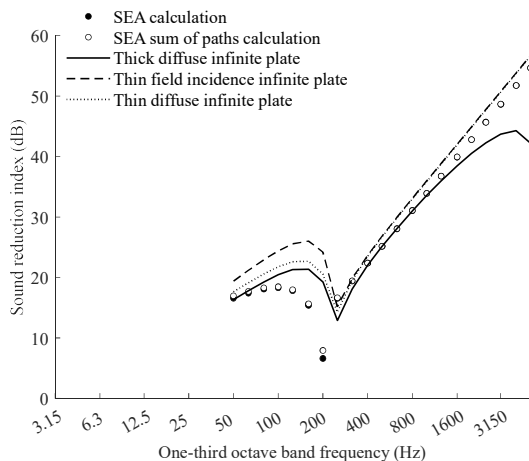


Figure 9. Sound insulation for the CLT plate.

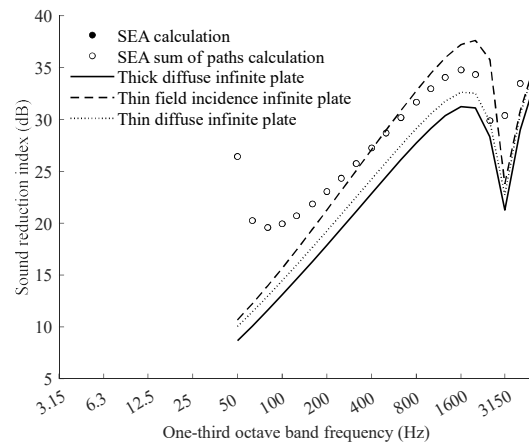


Figure 11. Sound insulation for the Perspex plate.

#### 5. CONCLUSION

The early results are presented for our hybrid model. The  $\eta_{12}$  and  $\eta_{23}$  loss factors are replicated using the hybrid method, however unlike the traditional method a  $\eta_{13}$  loss factor is obtained over the whole frequency range (not just below the critical frequency,  $f_c$ ). The meaning of this loss factor above the critical frequency ( $f > f_c$ ) is unclear. Further work would be required to extend the upper frequency range of the model. Future work is also required to improve accuracy and fully include a deterministic system in the model.

## 6. ACKNOWLEDGMENTS

This work is funded by a UKRI funded MSCA mobility fellowship (grant reference EP/X022021/1).

## 7. REFERENCES

- [1] R. S. Langley, J. A. Cordioli: “Hybrid deterministic-statistical analysis of vibroacoustic systems with domain coupling on statistical components,” *Journal of Sound and Vibration*, 321, pp. 893–912, 2009.
- [2] P. J. Shorter, R. S. Langley: “On the reciprocity relationship between direct field radiation and diffuse reverberant loading” *The Journal of the Acoustical Society of America*, 117, 85, 2005.
- [3] R. S. Langley: “Numerical evaluation of the acoustic radiation from planar structures with general baffle conditions using wavelets,” *The Journal of the Acoustical Society of America*, 121, 766, 2007.
- [4] L. Cremer, M. Heckl, B. A. T. Petersson: *Structure borne Sound – Structural Vibrations and Sound Radiation at Audio Frequencies*, (3<sup>rd</sup> edition), Springer 2005
- [5] C. Hopkins: *Sound Insulation*. Butterworth-Heinemann, City: Oxford, 2012.
- [6] R. J. M. Craik: *Sound Transmission Through Buildings Using Statistical Energy Analysis*, Gower Publishing Ltd., Aldershot 1996.
- [7] F. G. Leppington, K. H. Heron, E. Broadbent and S. M. Mead, “Resonant and non-resonant acoustic transmission of elastic panels; Part I the radiation problem,” *Proceedings of the Royal Society of London Series A, Mathematical and Physical Sciences*, pp. 309–337, 1987.
- [8] F. G. Leppington, K. H. Heron, E. G. Broadbent, S. M. Mead: “Resonant and non-resonant acoustic properties of elastic panels II. The transmission problem,” *Proceedings of the Royal Society of London Series A, Mathematical and Physical Sciences*, 412, pp. 309–337, 1987.